

The Influence of Shape on Ordering of Granular Systems in Two Dimensions

I.C. Rankenburg and R.J. Zieve

Physics Department, University of California at Davis

We investigate ordering properties of two-dimensional granular materials using several shapes created by welding ball bearings together. Ordered domains form much more easily in two than in three dimensions, even when configurations lack long-range order. The onset of ordered domains occurs near a packing density of 0.8, a phenomenon observed previously for disks. One of our shapes, the trapezoid, has packings that remain disordered and near the transition density even after annealing by shaking. Since random packings are unstable for disks and many other shapes in two dimensions, trapezoid packings provide a new approach to studying two-dimensional randomness. We also find that the rotational symmetry of a shape is an excellent predictor of how easily it orders, and a potential guide to identifying two-dimensional shapes that remain random after annealing.

PACS numbers: 45.70Cc, 81.05 Rm

I. INTRODUCTION

Granular materials are studied in materials science, geology, physics, and engineering. Their unusual dynamical behavior has attracted much recent attention, but even their most basic static properties are not yet understood [1, 2]. For example, a collection of uniform spheres in three dimensions reaches a final arrangement known as random close packing (RCP). The RCP density is 0.64, substantially smaller than the 0.74 density of the fcc and hcp lattices. The RCP density is robust to changes in the vibration method, or to using uniaxial or hydrostatic pressure to push the grains together [3]. Computer simulations also agree well with physical experiments [4]. The structure of RCP arrangements is thoroughly documented by experiments and simulations, but neither the arrangements nor their density is understood from fundamental principles. The only algorithms for generating an RCP configuration involve a simulated shaking procedure. Even attempts to derive the RCP density begin from experimentally measured correlation functions [5].

As a further complication, direct applications of packing densities often deal with non-spherical particles, or mixtures of shapes or sizes. In mixing dyes, the highest possible percentage of colorant depends on the RCP density for the molecule's shape [6]. In making ceramics, particles form clusters whose shape affects the final density [7]. Particle shape influences packing densities in complicated ways. The ideal maximum packing density, as well as the RCP density, depends on shape and is unknown in most cases. Furthermore, the density observed in a given experiment also depends on how easily particles move past each other into optimal positions. Interparticle friction can be large when a shape has flat sides, and multiple contacts can eliminate much of the particles' rotational freedom. Cubes, for example, have maximum packing density of 1 but reach a density of only 0.68 on deposition [8]. On the other hand, irregularly shaped particles are less dense than spheres on initial deposition but compress

particularly well with vibration [9].

Theoretical work has concentrated on packings of hard spheres [4, 5], with generalizations to hard ellipsoids [10, 11, 12, 13] or mixtures of sphere sizes [14, 15]. For ellipsoids, simulations find several phases as a function of particle density. Theory has rarely dealt with other shapes, even "simple" ones such as regular polygons and polyhedra. Without understanding the mechanisms by which such particles move into position, the utility of simulations is unclear.

For many physics issues, solving an analogous problem in two dimensions can provide insight to the full three-dimensional question. However, there is no stable random configuration of circles in two dimensions. Uniform spheres confined to a single layer easily form a triangular lattice, the densest possible packing. Experiments and simulations do suggest a transition between random and ordered configurations near a density of 0.80 [16, 17, 18]. Density increases much more slowly beyond this point. The number of touching disks in the configuration also changes sharply with density near 0.80. However, without a better definition of a "random" arrangement, pinpointing the exact transition and analyzing two-dimensional random close-packed configurations is impossible.

Not only spheres, but even unusual shapes such as regular pentagons anneal to their densest known packing in two dimensions [19]. The arrangement for pentagons is a double lattice, in which translates of a two-pentagon unit cover the plane. Computer simulations find an analogous double lattice for heptagons as well [20]. Thus these shapes too are impractical for studying random close packed structures.

Here we study several shapes in two dimensions. A main goal is to find shapes that remain disordered, which would lend themselves to studies of random arrangements. In addition, we may better understand the dependence of ordering properties on shape. Finally, packing in two dimensions is important in its own right in the behavior of films and monolayers.

All our shapes are clusters of spheres welded into triangu-

lar lattice positions. This guarantees that the densest packing is always a triangular lattice of the component spheres. The point contacts between clusters minimize friction and blocking effects as the shapes move past each other. Another advantage is that comparison with computer experiments is possible, since overlaps are easy to check with spheres. Visualizing the entire arrangement is also far easier in two dimensions than in three.

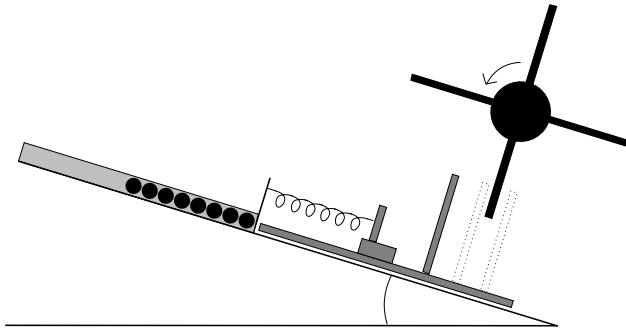


FIG. 1: A schematic of the experiment. Moving the arm of the sliding piece to one of the outlined sites changes the spring tension at the moment of release and hence the hit magnitude.

II. PROCEDURE

We welded together $\frac{1}{8}$ -inch diameter carbon steel ball bearings with a Unitek 60 welder set at its maximum power, 60 Watts. During the welding the balls were held in a bakelite mount machined to give the desired final shape. The shapes made were doubles, triples (three balls in a straight line), triangles of three or six balls, diamonds of four balls, trapezoids of five balls, and hexagons of seven balls. The welding appears not to distort the balls. One of the most stringent tests is that, as we shall see, several of the welded shapes order into perfect triangular lattices of their individual balls. A significant distortion from the welding would destroy the long-range order.

A schematic of our shaking apparatus is shown in Figure 1. Two pieces of plexiglas separated by 0.135-inch spacers confine balls inside to a single layer. The container is placed at an angle to the horizontal so that gravity pulls the balls towards one side. We typically fill a 9 inch by 4 inch region with ball clusters. Roughly 2500 single balls fit in this space. After putting the shapes in, we shake the box roughly to create a disordered initial state. An aluminum plate, connected to the plexiglas by a spring, serves as a hammer. Rotating spokes pull back and release the aluminum plate. On release, it strikes the bottom of the container and shakes the balls. A hit occurs once every three seconds for one hour. The balls stop moving completely between hits. The configuration changes substantially during the first few shakes, and negligibly at the end of the hour, but we have not investigated quantitatively the rate of ordering.

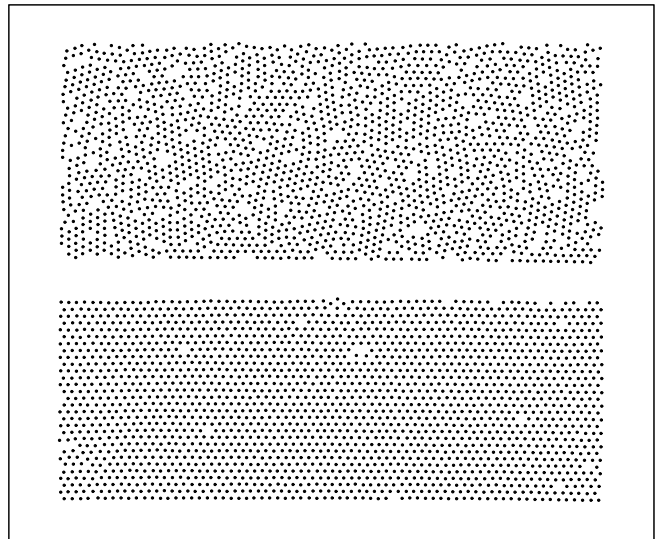


FIG. 2: The centers of the balls, as identified by the computer from digital photographs of a trapezoid initial condition (top) and a well ordered arrangement of doubles (bottom).

We vary both the maximum spring extension and the angle of the container. These parameters change the relative strengths of three physical forces: the hit magnitude, the component of gravity pulling the balls together, and the friction force between the balls and the plexiglas. Friction and effective gravity depend only on the angle, with friction decreasing as the angle becomes steeper and gravity increasing. We use eighteen different settings involving three spring extensions and seven angles between 20° and 50° .

The hit magnitude depends on both spring length and angle, since the weight of the striking plate itself changes the equilibrium length of the spring by an angle-dependent amount. A very hard hit destroys the memory of the situation, and each time the balls settle from scratch. Furthermore, very strong hits can break the weld joints. On the other hand, a hit so light that the displacement of the balls is small compared to the ball diameter makes rearrangement difficult and slow. In addition, for light hits at the smallest angles shapes occasionally stop moving in positions that clearly should be unstable, held in place only by friction. Thus we might expect an optimum hit magnitude, not necessarily the same for different shapes. Using a range of parameters lets us determine not only whether but also how easily different shapes order.

When the shaking finishes, we photograph the final configuration with an Olympus 340R digital camera and transfer the image to a computer. The computer scans the photograph for local bright spots, which appear near the center of each ball. We refine the positions with a weighted average of the pixels surrounding the bright spots. Figure 2 shows the computer's identification of an initial state and a well-ordered final state. To locate the balls successfully by this method, a single bright light source is used when taking the photograph. Multiple sources can lead to several bright spots on a single ball, or spots far from the ball center. A significant systematic er-

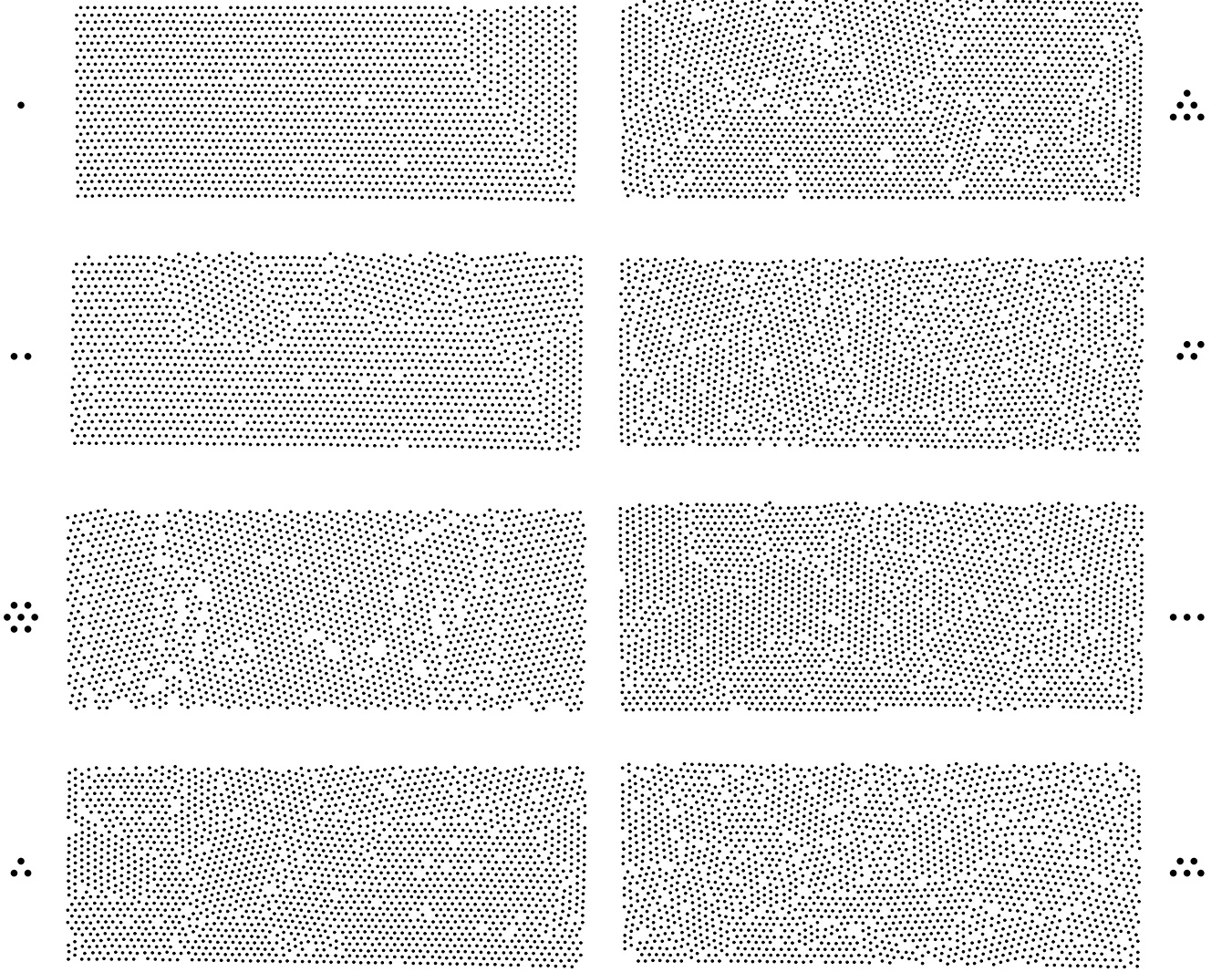


FIG. 4: Final configurations for different shapes for an angle of 40° and intermediate spring setting. Left, top to bottom: singles, doubles, hexagons, small triangles. Right, top to bottom: large triangles, diamonds, triples, trapezoids.

ror comes from warping of the photograph by the camera lens itself. To eliminate the warping, we generate a perfect triangular lattice of black dots on white paper and photograph it. We then find the displacement from ideal lattice sites of each photographed dot and interpolate to get the displacement at other points in the picture. Figure 3 shows the resulting vector field of displacements. We adjust the position of each ball center in the photographs to compensate for the warping. The maximum correction is comparable to one ball diameter.

After each trial we sort the shapes and verify that less than 7% of the shapes broke. The amount of breakage correlates strongly to both hit strength and shape. There is usually no breakage until mid-level hits and less than 3% on all but the hardest few settings. Shapes such as 3-ball triangles, with each ball welded to two neighbors, are strong. Triples, with two balls held by a single weld, break much more easily. Breakage seems to have little effect on the ordering. For all shapes, the run with the most breakage was not the one

with the best ordering. Even for triples, where broken shapes become singles and doubles, which both order easily, high breakage did not correlate to good order. A few settings for triples and 6-ball triangles, and one for doubles, were omitted because of large amounts of breakage.

III. RESULTS

As we vary the shaking parameters, all shapes except trapezoids and triples form domains comparable in size to the container itself, but they do so under increasingly restrictive hit conditions. Figure 4, which shows final configurations for parameters away from optimum, reveals the substantial differences among shapes and illustrates many of the trends we find. The arrangements all come from a 40° angle and the middle of the three spring settings. Singles, doubles and hexagons

TABLE I: Highest and lowest density for different shapes. The numbers in parentheses show what the densities would be if the holes were filled in.

	Highest			Lowest			Initial
Doubles	0.908 (0.912)	0.908 (0.911)	0.905 (0.909)	0.876 (0.881)	0.870 (0.875)	0.865 (0.873)	0.825
Hexagons	0.887 (0.895)	0.886 (0.894)	0.878 (0.891)	0.833 (0.861)	0.832 (0.850)	0.801 (0.829)	0.784
Small Triangles	0.881 (0.892)	0.879 (0.889)	0.877 (0.887)	0.848 (0.861)	0.845 (0.855)	0.844 (0.853)	0.820
Large Triangles	0.863 (0.883)	0.861 (0.880)	0.854 (0.872)	0.830 (0.842)	0.829 (0.839)	0.827 (0.837)	0.813
Diamonds	0.853 (0.880)	0.852 (0.870)	0.851 (0.869)	0.820 (0.832)	0.814 (0.822)	0.808 (0.814)	0.793
Triples	0.862 (0.874)	0.861 (0.873)	0.859 (0.870)	0.835 (0.841)	0.816 (0.823)	0.813 (0.816)	0.792
Trapezoids	0.839 (0.864)	0.836 (0.853)	0.832 (0.852)	0.812 (0.826)	0.809 (0.824)	0.808 (0.819)	0.788

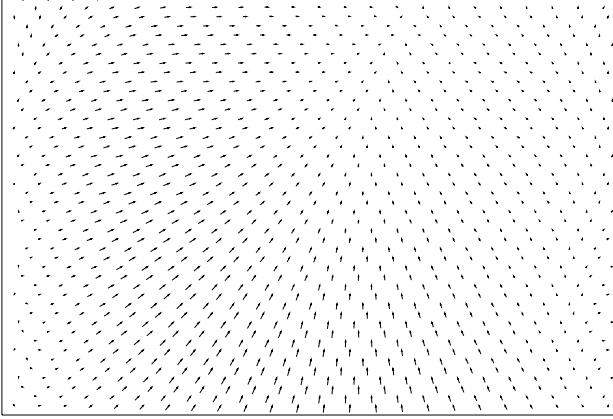


FIG. 3: This vector field shows the displacements from true positions due to the photographs. The entire region is roughly 70×30 ball diameters.

can form essentially perfect lattices, with a few large domains oriented by the container walls. For triangles and diamonds, small domains always appear in addition to the large ones. Domain sizes for triples and trapezoids are always substantially smaller than the container size, suggesting an absence of long-range order. Usually the best ordering occurs at an intermediate hit power. Trapezoids are an exception, with the degree of order nearly independent of hit settings.

In all the arrangements of Figure 4, the individual balls composing the shapes form ordered domains with sharp boundaries. The configurations have progressively decreasing domain sizes. As the domains shrink, interstitial clusters and regions that appear “random” increase in size and number. Much of the configuration for trapezoids, the least ordered shape, has ordered regions no more than 6 balls (or two

trapezoids) across. This small domain size suggests that trapezoids approach a regime of stable random arrangements. We stress that our notion of “order” involves only the arrangement of the individual spheres. Identifying which balls are welded together is difficult. We have done so for a few cases and find no long-range orientational order beyond the requirement that the individual balls lie in a lattice. Thus we are really studying the packing of disks in a plane subject to certain constraints.

The shapes also differ in the voids that appear. Triples give rise to fewer holes than do the non-linear shapes. Larger shapes support larger holes, sometimes with characteristic shapes. For example, hexagon packings regularly show hexagonal holes, and the large (6-ball) triangles often have three balls missing in a triangular pattern. Hexagons frequently have rows of holes, as on the far left of Figure 4, as well as substantial void regions at crystallite boundaries.

IV. LARGE-SCALE ORDER

We quantify the degree of order in several ways. Density, shown in Table I, measures the state of the entire system. We use a large rectangle and calculate the total ball area inside, contributed both by balls completely inside and by balls on the boundary. Our biggest source of error in the density calculation comes from the lengths of the rectangle’s sides in units of ball diameters.

The densities confirm the qualitative discussion on the relative ordering of the different shapes in Figure 4. Of the two main defects in our arrangements, holes and grain boundaries, holes have a much larger effect on density, particularly for the largest shapes. Revised densities, treating holes in an otherwise crystalline region as filled, are shown in parentheses in Table I. Small triangles pack slightly better than large triangles, although the difference decreases when holes

are counted as filled. The similar behavior of the two sizes of triangles, particularly after discounting holes, shows that the ordering behavior is not completely dominated by size-dependent effects such as the container size or hit power.

The density of a perfect triangular lattice, and the maximum possible density for all of our shapes, is 0.9069. (That the densest packings for doubles in Table I apparently exceed this value is merely a consequence of the uncertainty in the density calculation. There may be a systematic error of less than 0.5% toward larger density, perhaps because the container height is slightly larger than the ball diameter and the balls may not lie perfectly flat.) For packing of spheres in two dimensions, a transition from random to ordered structures occurs near 0.80. In one experiment a gradual, uniform contraction of a rubber sheet increases the density of disks lying on the sheet [17]. After the disks come into contact, they slide across the sheet under further contraction. The disk motion from sliding causes hexagonal crystals to form at a density of about 0.82. Another technique [16] shakes a fixed-density system to find the most probable configurations. Repeating with a series of densities shows a change in behavior near 0.75, with large lattice regions forming above this density. Computer simulations of a liquid-solid interface have put a hard-sphere liquid near a two-dimensional lattice of attractive sites and find a possible first-order transition due to packing effects at a density 0.72 [18]. The restriction to lattice sites naturally reduces the transition density.

Interestingly, our lowest densities, found for trapezoids, are

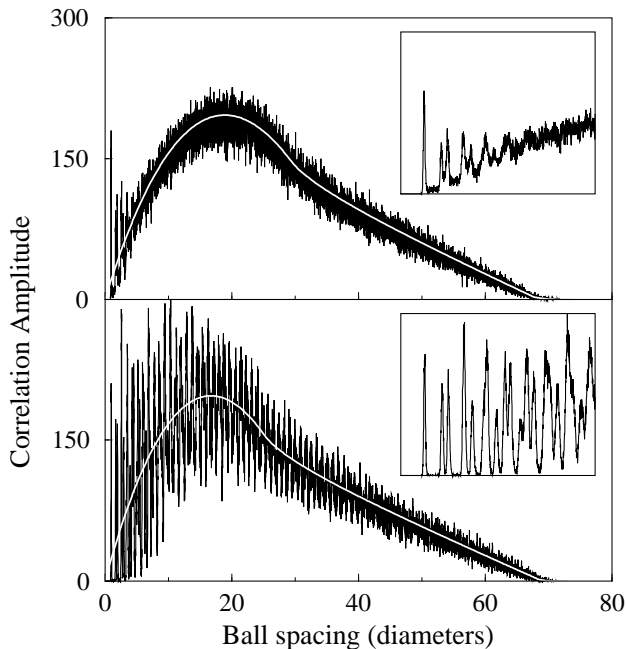


FIG. 5: Pair correlation functions corresponding to the two-ball configurations of Figure 2. The white lines are average values calculated from Eqs. (1)-(3), as described in the text. The insets expand the regions from zero to eight ball diameters.

very close to the transition density, and qualitatively there appear to be only small domains in these packings. The agreement of the trapezoid density with the previously observed hard-disk transition density supports the idea of using final trapezoid arrangements as models of two-dimensional RCP configurations. Although the exact configurations attained by trapezoids would be unstable as arrangements of unwelded single balls, the maximum random density should be similar for the two cases. The perfect alignment of the balls within each trapezoid increases the maximum random density, but the larger holes in trapezoid packings decrease the density.

The comparison with the less well-ordered configurations also illustrates how easily different shapes order. Even with very light taps, doubles order reasonably well, for instance. Not surprisingly, the degree of order under light taps has strong correlation to the size of the shapes used.

To identify a length scale for the domains in each arrangement, we calculate a two-ball correlation function. We consider the distance between each pair of balls and construct a histogram of these distances, with about 320 bins per ball diameter. This is equivalent to finding the number of ball centers in annuli of fixed width centered at a single ball. For a perfect lattice, the result is sharp peaks at spacings characteristic of the triangular lattice: $1, \sqrt{3}, 2$, etc. diameters. Imperfections, both in the identification of the ball centers and in the lattice itself, broaden the peaks and raise the heights of the intervening values. Figure 5 shows the histograms corresponding to the lattices of Figure 2.

Geometrical considerations determine the average shape of the histogram. The linear increase in average amplitude with distance at small separations corresponds to the increase in the circumference of a circle with its diameter. The average amplitude in the histogram falls off at larger distances because of the finite size of our sample. We calculate the exact distribution of separations for two balls randomly positioned in a rectangle, as follows.

Let a and b be the lengths of the rectangle's sides, with

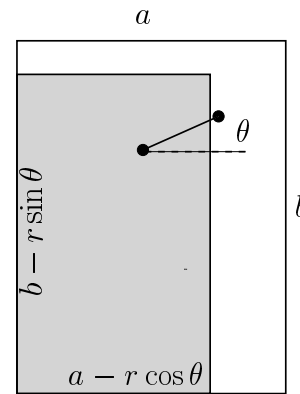


FIG. 6: Geometry of the average histogram calculation described in the text. If two points in the larger rectangle have the angle and separation shown, the lower left point always lies within the shaded region.

TABLE II: Extent of order, in ball diameters. The length scale of the most ordered arrangements is limited by the sample size.

	Most ordered			Least ordered			Initial
Doubles	30.2	27.7	27.0	14.3	13.0	10.2	3.0
Hexagons	28.0	25.5	25.1	7.8	7.6	7.5	3.3
Small Triangles	25.3	22.1	20.4	8.1	8.0	7.7	2.7
Large Triangles	20.6	14.5	13.8	7.9	6.8	6.8	2.7
Diamonds	13.6	13.1	11.7	4.6	4.6	3.7	3.0
Triples	12.2	10.2	8.1	4.5	3.0	2.0	2.0
Trapezoids	6.0	6.0	5.6	4.3	3.7	3.6	2.5

TABLE III: D , a weighted ratio of the first few peak and valley amplitudes in the two-ball correlation function. See text.

	Highest			Lowest			Initial
Doubles	1480	1451	642.6	78.7	76.2	64.2	16.0
Hexagons	410.8	216.8	191.0	54.2	42.3	33.6	26.7
Small Triangles	109.2	105.3	104.7	43.1	42.9	40.8	20.5
Large Triangles	91.8	88.6	82.4	44.2	38.9	35.0	25.3
Diamonds	71.0	68.7	61.8	26.5	23.9	20.3	18.6
Triples	57.6	50.5	44.4	23.6	17.9	16.2	14.1
Trapezoids	43.1	35.6	32.9	24.7	24.5	21.5	20.1

$a \leq b$. The region of phase space corresponding to choosing two points at random in the rectangle has volume $(ab)^2$. Now calculate the volume of the subset with point separation between r and $r + dr$. With the rectangle oriented as in Figure 6, the first point lies below and to the left of the second point one quarter of the time. Let θ be the angle between the line connecting the points and the rectangle's short side. If $r \leq a \leq b$, the first ball can lie anywhere inside the shaded rectangle, of sides $a - r \cos \theta$ and $b - r \sin \theta$. Integrating over θ , the volume corresponding to separation r to $r + dr$ is

$$rdr \int_0^{\pi/2} d\theta 4(a - r \cos \theta)(b - r \sin \theta) \quad (1)$$

$$= [2\pi ab - 4(a + b)r + 2r^2]rdr.$$

For $a \leq r \leq b$, the same integral applies, except that not all angles are allowed. The result is

$$4rdr \int_{\cos^{-1} \frac{a}{r}}^{\pi/2} d\theta (a - r \cos \theta)(b - r \sin \theta) = \quad (2)$$

$$[2\pi ab - 4ab \cos^{-1} \frac{a}{r} - 2a^2 - 4b(r - \sqrt{r^2 - a^2})]rdr.$$

Finally, for $a \leq b \leq r \leq \sqrt{a^2 + b^2}$, there is an additional restriction on the allowed θ , giving

$$4rdr \int_{\cos^{-1} \frac{a}{r}}^{\sin^{-1} \frac{b}{r}} d\theta (a - r \cos \theta)(b - r \sin \theta) = \quad (3)$$

$$[4ab(\sin^{-1} \frac{b}{r} - \cos^{-1} \frac{a}{r}) + 4a\sqrt{r^2 - a^2}$$

$$+ 4b\sqrt{r^2 - a^2} - 2(a^2 + b^2 + r^2)]rdr.$$

These formulas, divided by $(ab)^2$, give the probability that two points are separated by a distance between r and $r + dr$.

For a region containing N balls, the average value of the pair correlation function is this function times the number of pairs, $\binom{N}{2}$. The white lines of Figure 5 are the average values calculated in this way.

The two parts of Figure 5 differ most obviously in the extent of the structure. In the upper graph, peaks give way to noise near 4 ball diameters, whereas the lower graph retains structure to 40 diameters. To measure the long-range correlations, we begin by taking the difference between the observed histogram and its calculated average value. We average the 50 highest values within a window 2 ball diameters wide, and also the 50 lowest values. Then we take the difference between the two. As the window moves to larger distances, this difference generally decreases. It approaches 50 for the largest distances, with extremely disordered lattices reaching this value within a few ball diameters. To assign a length scale to a configuration, we set a cutoff of 80. The best lattices drop below 80 near 30 ball diameters, which is comparable to the system size in one direction. Even primarily crystalline arrangements often have two or three domains, aligned with the different walls of the container, and the length scale we find depends on the relative sizes of these domains. The length scales for several different configurations are shown in Table II.

V. LOCAL ORDER

To further characterize the appearance of holes and grain boundaries in the different shapes, we analyze short-range order using methods sensitive to each type of imperfection. Domain boundaries strongly influence the short-distance region

of the two-ball correlation function, while coordination numbers are more sensitive to voids.

We use the correlation function out to 3 ball diameters. We add the heights of the first five peaks, and divide by the sum of the first and third valley heights. We omit the second and fourth valleys because they lie between closely spaced peaks and give less consistent results. This quotient D is larger for better ordered configurations. For perfect order, no balls lie in the valleys and the ratio is infinite. For the most disordered system we can engineer, the value is about 20. Using a ratio means that the exact number of balls used for each shape is unimportant.

Values for best, worst, and initial arrangements appear in Table III. This probe is very sensitive to grain boundaries. The two most ordered runs of doubles have a single crystal spanning the entire container. The third run has two regions with a grain boundary between them, which greatly reduces the peak-to-valley ratio. The best hexagon run has one large domain and a small second domain, while the other runs have several small domains in addition to the large one. In fact, as shown in Figure 7, for systems with a single domain boundary the peak-to-valley ratio is proportional to the length of the boundary. With more than two domains this linear relationship fails, but the high sensitivity of the peak-to-valley ratio to boundaries remains.

Voids, interstitials, and other imperfections generally have much less effect than boundaries. One exception is that in nearly perfect lattices, the first few valleys drop so close to zero that any disorder changes their relative levels substantially; this causes the wide variation in the numbers shown for doubles. A second exception is that occasionally, particularly with doubles, a square lattice forms in a small area. This produces a peak on the histogram at $\sqrt{2}$ diameters, which is close to the center of the first valley and can have a particularly large effect.

Doubles and hexagons show the best ordering, as they do

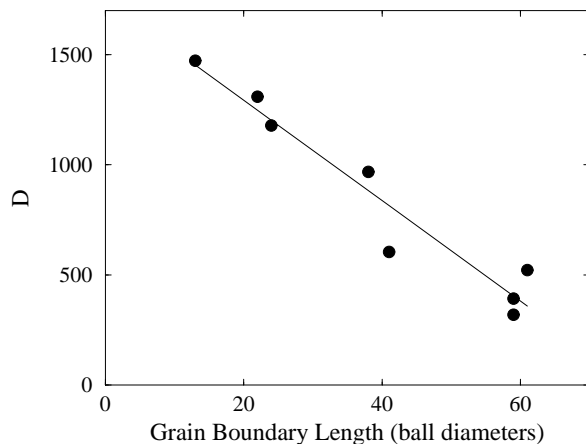


FIG. 7: D , a ratio of correlation function values described in the text, as a function of boundary length, for lattices perfect except for a single grain boundary. The line is a least-squares fit.

by the long-range measures. Once again, the two sizes of triangles are very similar in both the best and worst order displayed. One of the clearest indications of the sensitivity of this index to grain boundaries is the noticeable difference between diamonds and triples. The two shapes have comparable densities once voids are filled in, and have visually similar amounts of ordering. However the triples definitely have more grain boundaries, with fewer interstitials, which is reflected here.

Properly normalizing for the order inherent in the different shapes is a difficult problem. Resolving the effect of internal correlations among the balls composing a shape is particularly difficult with this measurement. The initial ordering corresponds well to cluster size, suggesting that the internal correlations are important here. However, this correlation disappears after shaking, even for the least effective hit parameters. We emphasize the similarities between the two triangle shapes as evidence that this factor is unimportant in the results from the final configurations.

As a complementary local order indicator, we calculate the Voronoi region of each ball. The Voronoi region of a ball consists of the points closer to that ball than to any other. The edges of the region are perpendicular bisectors of the lines connecting the ball to its neighbors, so for a perfect triangular lattice every Voronoi region would be a regular hexagon. Pentagonal or heptagonal regions signify defects in the lattice. To measure order, we find the percentage of balls with six-sided Voronoi regions. This tells us how many balls are in the interior of some domain.

The highest percentage of hexagonal Voronoi regions ranges from over 98% for doubles to 78% for trapezoids. The highest, lowest, and initial percentages for each shape appear in Table IV. These three numbers differ by at most 3.5% for a single shape, and usually by less than 1%. For comparison, the values for a typical initial configuration and for the most disordered final arrangements are also shown. Doubles order the most easily. Hexagons achieve the next highest order, although at the poorest hit settings they remain more disordered than triangles. Of the remaining shapes, triples and diamonds have six nearest neighbors with about the same frequency. Trapezoids have significantly more irregular Voronoi regions.

We next address the issue of correlations within the larger shapes. The initial configurations given in Table IV show no trend of higher order for larger clusters. The differences among the final configurations also exceed correlation effects. For example, each hexagon has a center ball with six nearest neighbors, and centers account for 14.3% of all balls. For the three most ordered hexagon configurations, on average 94.5% of the balls have six nearest neighbors, so 5.5% do not. Since all the center balls do, 6.4% of the non-centers must have imperfect Voronoi regions, a change of less than 1% in the number with hexagonal Voronoi regions. The difference between hexagons and triangles is several times this large, so the perfect arrangement around the center balls cannot explain the entire difference. The more complicated effects involve the outer balls. For a hexagon, each of the six outer balls has three nearest neighbors perfectly positioned. A large triangle has three balls with four nearest neighbors, and three oth-

TABLE IV: Percentages of balls with hexagonal Voronoi regions, for several shapes. The highest and lowest percentages among final packings, as well as the initial percentage, are shown.

	Highest			Lowest			Initial
Doubles	98.7	98.2	97.6	88.2	87.1	86.8	74.4
Hexagons	96.2	94.1	93.3	80.8	80.5	73.3	70.8
Small Triangles	89.9	89.5	88.6	82.1	82.0	82.0	73.1
Large Triangles	88.0	87.8	87.6	83.3	83.1	80.6	78.4
Diamonds	87.3	85.3	83.8	73.9	73.0	71.3	69.0
Triples	86.2	85.7	85.7	77.8	72.8	71.3	67.3
Trapezoids	78.1	78.1	77.6	71.7	71.5	70.8	67.4

ers with two. Without determining precisely the implications for the Voronoi region's shape, we posit that the effect should be much smaller than that of the central ball of the hexagon, and that we can reasonably ignore it in distinguishing among shapes. Also note that the hexagons form a very poorly ordered initial state, despite the automatically proper coordination number of the center balls.

The percentage of hexagonal Voronoi regions is particularly sensitive to holes. A single missing ball in a perfect lattice creates six pentagonal Voronoi regions, with larger holes disturbing more Voronoi regions. Slight lattice imperfections, such as those introduced by the ball center identification, usually reduce the number of non-hexagonal Voronoi regions around a single void to four. Grain boundaries have less effect, with typically one imperfect Voronoi region per ball of boundary

length. Interstitials have little effect beyond the balls that compose them, since the balls at the surface of a grain already have irregular Voronoi regions.

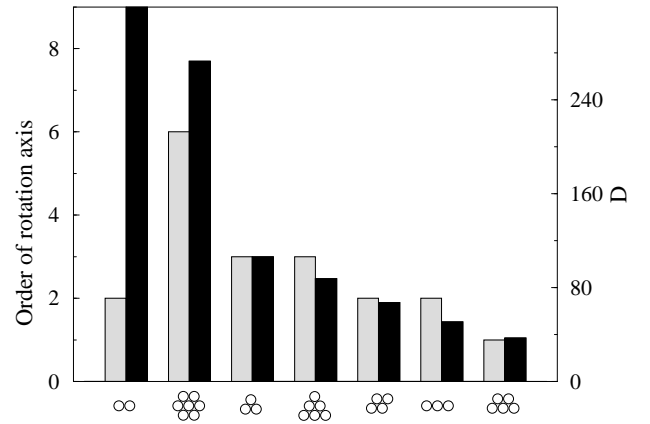


FIG. 9: A comparison of the average of the highest values D (right) and the number of symmetries (left) for each shape. For doubles D is actually 1191, far off the scale of this graph.

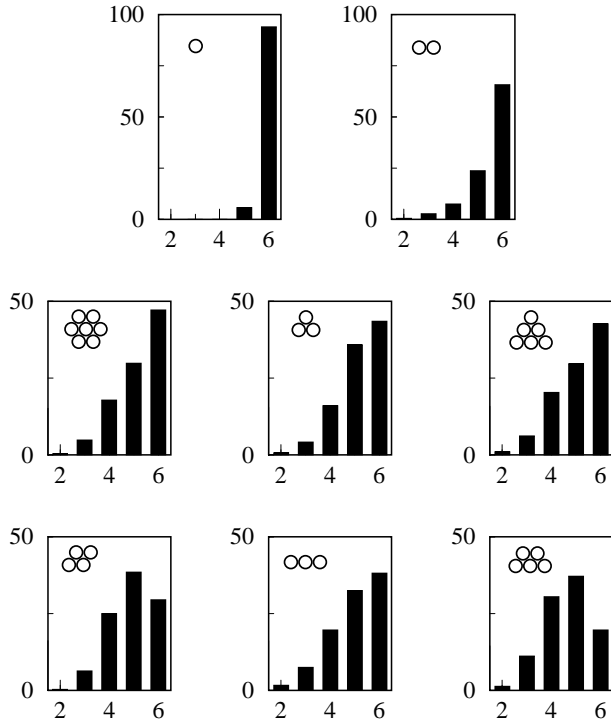


FIG. 8: Percentage of balls with a given coordination number, for the configurations of Figure 4.

The coordination number, the number of balls touching a given ball, is an indicator related but not identical to the Voronoi region shape. No coordination number can exceed six, although a Voronoi region can have more than six sides. Coordination numbers are also far more sensitive than Voronoi regions to small displacements of balls, for example from noise in identifying the ball centers. In Figure 8 we show the distribution of coordination numbers for the configurations of Figure 4. For random sphere arrangements in three dimensions, the coordination number distribution varies more than other properties [3], including the pair correlation function. Balls are taken as touching when their computer-identified centers lie within 1.08 ball diameters. We choose this as a cutoff because at longer distances significant asymmetry appears in the first peak of the two-ball correlation function.

Earlier two-dimensional experiments found a sharp change in average coordination number near the random-ordered transition [17]. Although our coordination numbers are larger due to correlations introduced by the welds, they decrease abruptly near the same density. The similar behavior gives further encouragement to the possibility of studying random arrange-

ments in two dimensions.

VI. ROTATIONAL SYMMETRY

We find that rotational symmetry is an excellent guide for predicting the degree of order that a shape supports. Figure 9 shows both the average of the three highest peak-to-valley ratios D (Table III) for each shape, and also the order of the rotational axis. Except for doubles, the correspondence is excellent. The various other measures of order would give similar results. The correspondence between ability to order and rotational symmetry suggests that domains grow around the edges. To join the ordered portion, a shape must have the correct orientation. Its rotational symmetry sets a limit on the maximum angle through which it needs to rotate to reach this orientation. On the other hand, the rotational symmetry has little correlation to the degree of order in the initial configurations, which do not depend on growth at domain edges.

Several features of the final packings make sense when considering domain growth. For some shapes, any stable position near a growing crystal is part of the lattice. For example, stability for doubles under gravity requires at least three contacts, not all on the same ball. At the edge of a crystalline region, only lattice sites satisfy this criterion. By contrast, triples do have a stable off-lattice location, as illustrated in Figure 10. Trapezoids and large triangles also have stable nonlattice positions for a single particle added to an existing lattice, but our other shapes do not. This may account for the significantly longer length scale of small triangles compared to large ones. For diamonds, also illustrated in Figure 10, clusters positioned incompatibly may lead to voids, explaining the large number of voids in diamonds (see Table I). Finally, doubles can generally join an ordered region in any of three distinct orientations, allowing them to order easily despite their lack of much rotational symmetry.

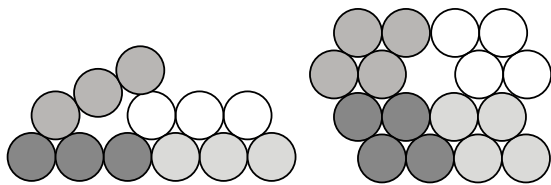


FIG. 10: Possible lattice growth with triples (left) and diamonds (right).

VII. CONCLUSIONS AND FURTHER WORK

We have studied how several shapes composed of welded spheres pack in two dimensions. Our goals were to understand how particle shape affects packings, and especially to identify two-dimensional random close-packed configurations. Constructing shapes as sphere clusters avoids issues of maximum density and interparticle friction changing with shape, and

permits detailed comparison of the configurations reached by different shapes. One consequence is that we find a strong correlation between the rotational symmetry of a particle and its short-range order. In addition, the defects in long-range order relate to geometry. Shapes where at least one side is three balls long produce more grain boundaries, while voids are common with large nonlinear shapes.

In keeping with the tendency of shapes to order in two dimensions, most of our clusters can anneal into configurations with long-range order of the individual spheres. Even under conditions where no long-range order appears, the shapes form small domains with sharp boundaries, qualitatively different from the random configurations that appear in three dimensions. Trapezoids are the one exception. All their packings remain random or nearly so, with typical domain sizes of only two trapezoids. Interestingly, the onset of ordered domains occurs near the packing density 0.8, where previous experiments on disks already showed evidence for a transition between random and ordered states.

Finding shapes such as trapezoids with stable random arrangements in two dimensions allows comparison to the packing behavior of spheres in three dimensions. We plan to pursue the similarities further by studying the time dependence of trapezoid configurations during annealing. The data on rotational symmetry suggest that examining elongated shapes with little symmetry may identify other shapes that do not crystallize. However, because of difficulties with breakage and with system size, this work is better done through computer simulations. The data presented here provide a series of test cases on the realism of any simulations.

Although our artificial particles are convenient for comparisons among the shapes, the unusual surface geometry clearly changes some behavior from that of similar but convex shapes. The irregular surfaces allow neighboring particles to lock together, leading to the high void densities for our larger shapes. More significantly, only the constituent spheres form ordered structures, *not* the larger shapes. For example, two-dimensional simulations of prolate ellipses under the influence of gravity find orientational but not translational long-range order [21]. By contrast, our doubles have no long-range orientational order. Instead, the dimples in the shapes' sides allow neighboring doubles to interlock and overcome the effect of gravity. A further project would deform doubles gradually into ellipsoids by filling in the dimples, while tracking changes in the characteristic arrangements. Once again, this project is most practical through simulations.

We are continuing work along other lines as well. Time dependence measurements for shapes that do crystallize may help in understanding how non-spherical particles move into position. Finally, we plan to extend the measurements towards three dimensions by varying the container thickness to accommodate more layers of balls.

VIII. ACKNOWLEDGEMENTS

We thank J.D. Lawton for help in setting up the apparatus. This work is supported by the National Science Foundation under DMR-9733898.

REFERENCES

- [1] R.M. German, *Particle Packing Characteristics* (Metal Powder Industries Federation, Princeton, 1989).
- [2] D.J. Cumberland and R.J. Crawford, *The Packing of Particles* (Elsevier, Amsterdam, 1987).
- [3] J.D. Bernal and J. Mason, "Coordination of Randomly Packed Spheres," *Nature*, **188**, 910 (1960).
- [4] W.S. Jodrey and E.M. Tory, "Computer Simulation of Close Random Packing of Equal Spheres," *Phys. Rev. A* **32**, 2347 (1985).
- [5] J.G. Berryman, "Random Close Packing of Hard Spheres and Disks," *Phys. Rev. A* **27**, 1053 (1983).
- [6] G. Bierwagen, R. Fishman, T. Storsved, and J. Johnson, "Recent Studies of Particle Packing in Organic Coatings," *Prog. Organic Coatings*, **35**, 1 (1999).
- [7] J.C. Kim, K.H. Auh, and D.M. Martin, "Multi-level Particle Packing Model of Ceramic Agglomerates," *Modelling Simul. Mater. Sci. Eng.* **8**, 159 (2000).
- [8] J.M. Coulson, "The Flow of Fluids Through Granular Beds: Effect of Particle Shape and Voids in Streamline Flow," *Trans. Inst. Chem. Engr.*, **27**, 237 (1949).
- [9] R. Meldau and E. Stach, "The Fine Structure of Powders in Bulk with Special Reference to Pulverised Coal," *J. Inst. Fuel* **7**, 336 (1934).
- [10] J.A. Cuesta and D. Frenkel, "Monte Carlo Simulation of Two-Dimensional Hard Ellipses," *Phys. Rev. A* **42**, 2126 (1990).
- [11] J. Vieillard-Baron, "Phase Transitions of the Classical Hard-Ellipse System," *J. Chem. Phys.* **56**, 4729 (1972).
- [12] B.J. Buchalter and R.M. Bradley, "Orientational Order in Amorphous Packings of Ellipsoids," *Europhys. Lett.* **26**, 159 (1994).
- [13] J.D. Sherwood, "Packing of Spheroids in Three-Dimensional Space by Random Sequential Addition," *J. Phys. A: Math. Gen.* **30**, L839 (1997).
- [14] H.H. Kausch, D.G. Fesko, and N.W. Tschoegl, "The Random Packing of Circles in a Plane," *J. Colloid Interface Sci.* **37**, 603 (1971).
- [15] A.S. Clarke and J.D. Wiley, "Numerical Simulation of the Dense Random Packing of a Binary Mixture of Hard Spheres: Amorphous Metals," *Phys. Rev. B* **35**, 7350 (1987).
- [16] D. Turnbull and R.L. Cormia, "A Dynamic Hard Sphere Model," *J. App. Phys.* **31**, 674 (1960).
- [17] T.I. Quickenden and G.K. Tan, "Random Packing in Two Dimensions and the Structure of Monolayers," *J. Colloid Interface Sci.* **48**, 382 (1974).
- [18] E. Kierlik and M.L. Rosinberg, "The Role of Packing Effects at a Liquid-Solid Interface: A Model for a Surface Transition," *J. Phys.: Condens. Matter* **2**, 3081 (1990).
- [19] Y. Limon Duparcmeur, A. Gervois, and J.P. Troadec, "Crystallization of Pentagon Packings," *J. Phys.: Condens. Matter* **7**, 3421 (1995).
- [20] Y. Limon Duparcmeur, A. Gervois, and J.P. Troadec, "Dense Periodic Packings of Regular Polygons," *J. Phys. I France* **5**, 1539 (1995).
- [21] B.J. Buchalter and R.M. Bradley, "Orientational Order in Random Packings of Ellipses," *Phys. Rev. A* **46**, 3046 (1992).